

Progress in year 1999

1. Strongly enhanced inelastic collisions in a Bose-Einstein condensate near Feshbach resonances

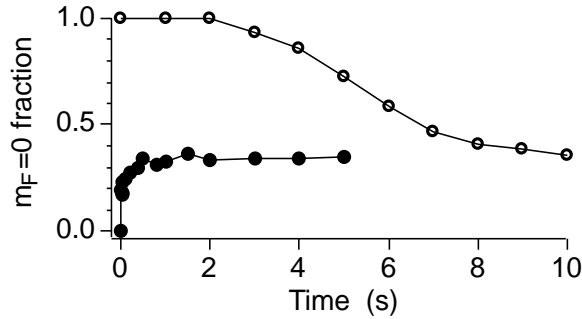
The properties of Bose-Einstein condensed gases can be strongly altered by tuning the external magnetic field near a Feshbach resonance. Feshbach resonances affect elastic collisions and lead to the observed modification of the scattering length. However, we found that this is accompanied by a strong increase in the rate of inelastic collisions. The observed three-body loss rate increased when the scattering length was tuned to both larger or smaller values than the off-resonant value [1]. The maximum measured increase of the loss rate was several orders of magnitude. Sweeps of the magnetic field through the resonance resulted in loss of most of the atoms in one microsecond. These observations are not explained by theoretical treatments and indicate molecular and many-body physics which is not yet accounted for. The strong losses impose severe limitations for using Feshbach resonances to tune the properties of Bose-Einstein condensates. A new Feshbach resonance in sodium at 1195 G was observed which has a region of negative scattering length on the low field side of the resonance which can therefore be directly approached without crossing any other resonance.

2. Metastable Bose-Einstein condensates

During the studies of the spinor ground states we encountered two different types of metastability which we investigated in more detail [2]. In one case, a two-component condensate in the $m_F=+1$, 0 hyperfine states was stable in spin composition, but spontaneously formed a metastable spatial arrangement of spin domains. In the other, a single component $m_F=0$ condensate was metastable in spin composition with respect to the development of $m_F=+1$, -1 ground-state spin domains. In both cases, the energy barriers which caused the metastability were much smaller than the temperature of the gas (as low as 0.1 nK compared to 100 nK) which would suggest a rapid thermal relaxation. However, since the thermal energy is only available to non-condensed atoms, this thermal relaxation was slowed considerably due to the high condensate fraction and the extreme diluteness of the non-condensed cloud.

When a condensate was initially prepared in a pure $m_F=0$ state metastability of up to 5 sec was observed for the formation of the equilibrium spin domain structure (see figure). In contrast when the system was prepared in an equal mixture of $m_F=+1$ and $m_F=-1$ atoms the fraction of atoms in the $m_F=0$ state grew without delay, arriving at equilibrium within just 200 ms.

Metastability of the spatial distribution was observed in a system of $m_F=+1$ and $m_F=0$ atoms. After the $m_F=0$ state was populated with an rf pulse, the system rapidly developed into alternating layers of $m_F=0$ and $m_F=1$ spin domains of about 40 μm in thickness which were metastable for 20 seconds in the absence of magnetic field gradients.

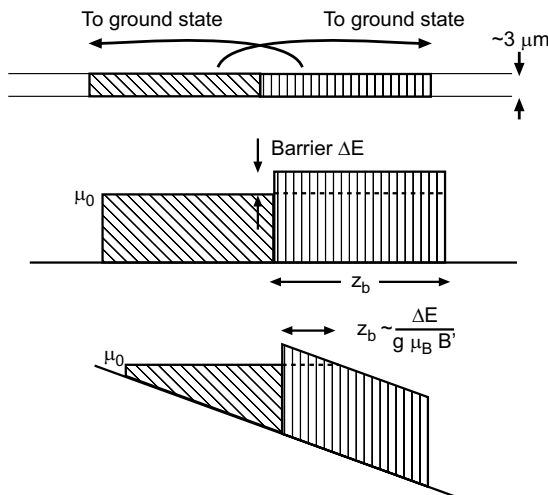


Metastability of the pure $m_F = 0$ state in the presence of a magnetic bias field (250 mG) and gradient (44 mG/cm). The evolution toward equilibrium of an initially pure $m_F = 0$ condensate (open symbols), and a mixture of $m_F = 1$ and $m_F = -1$ (closed symbols) is shown by plotting the fraction of atoms in the $m_F = 0$ state vs. dwell time in the optical trap.

3. Quantum tunneling across spin domains in a Bose-Einstein condensate

The observation of metastable spin domains in optically trapped $F=1$ spinor Bose-Einstein condensates of sodium [2] raised the question of how thermal equilibrium would ultimately be achieved. Besides thermally activated processes we observed quantum tunneling as equilibration process. For the study of this process, spinor condensates were prepared which consisted of only two spin domains in the $m_F=0$ and $m_F=+1$ states. Those domains are immiscible due to their antiferromagnetic interaction. When a field gradient was added which made it energetically favorable for the two domains to change sides, quantum tunneling was observed. A mean-field description of the tunneling process was developed and agreed well with the measurements [3].

The analysis showed that the tunneling rates are a sensitive probe of the boundary between spin domains, and indicated an unpredicted spin structure in the boundary between spin domains which is prohibited in the bulk fluid.



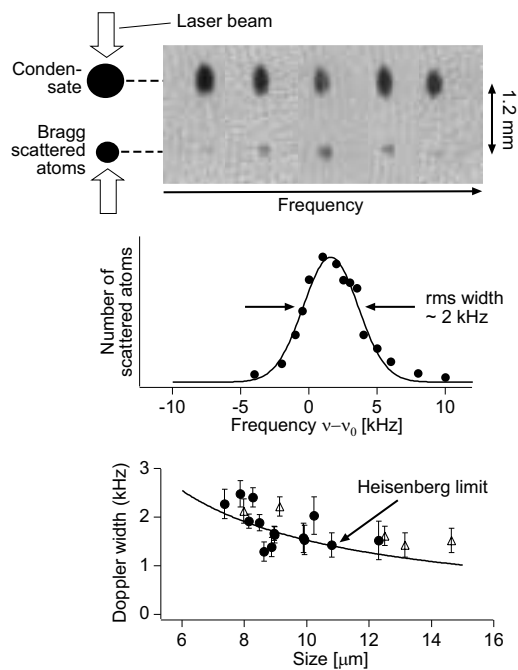
Study of quantum tunneling in a two-component Bose-Einstein condensate. The $m_F=1$ and $m_F=0$ (vertical hatch) atoms form two immiscible spin domains (upper figure) because the $m_F=1$ atoms experience an energy barrier due to the repulsive mean field interaction (middle figure). When a longitudinal magnetic field gradient is applied, the effective potential for the $m_F=1$ atoms changes to the lower figure, and the spin domains can rearrange themselves by quantum tunneling through each other.

4. Bragg spectroscopy of a Bose-Einstein condensate

The first evidence for Bose-Einstein condensation in dilute gases was obtained by a sudden narrowing of the velocity distribution as observed for ballistically expanding clouds of atoms. However, the dominant contribution to the observed momentum distribution of the expanding condensate was the released interaction energy (mean-field energy) resulting in momentum distributions much broader than the zero-point motion of

the ground state of the harmonic trapping potential. Since the size of a trapped condensate with repulsive interactions is larger than the trap ground state, the momentum distribution should be considerably narrower than in the trap ground state. We could measure the momentum distribution of a trapped condensate with Doppler velocimetry using two-photon Bragg scattering. We observed that the momentum distribution was Heisenberg uncertainty limited by its finite size, i.e. the coherence length of the condensate was equal to its size [4].

A shift of the narrow Bragg resonance was caused by the repulsive interactions within the condensate resulting in a spectroscopic measurement of the mean-field energy. More generally, we have established Bragg scattering as a spectroscopic technique to probe properties of the condensate. It can be used to map out the density fluctuations of the system and thus to measure directly the dynamic structure factor $S(q, \omega)$, which is the Fourier transform of the density-density correlation function and is central to the theoretical description of many-body systems.



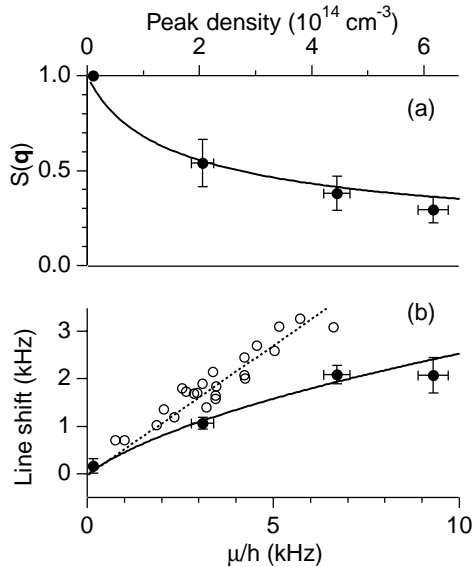
Bragg spectroscopy of a trapped condensate. A condensate was exposed to two counterpropagating laser beams and analyzed using time of flight absorption imaging (upper part). The number of Bragg scattered atoms showed a narrow resonance when the difference frequency between the two laser beams was varied (upper and middle part). The width of the resonance was studied for various radial sizes of the condensate. The solid line (lower part) compares the experimental results with the prediction for the momentum uncertainty due to the finite size.

5. Excitation of phonons in a Bose-Einstein condensate by light scattering

Light scattering imparts momentum to the condensate and creates an excitation (which can be a phonon or a free particle). A detailed study of the scattered light should therefore reveal a detailed picture of the Bose condensate similar to the case of superfluid helium where neutron scattering was used to obtain the spectrum of elementary excitations.

In previous work [4] we showed how a condensate responds to a large momentum transfer which lead to particle-like excitations. Light scattering at small angles does not impart enough momentum to the condensate to create a recoiling atom. Instead, it creates a sound wave by “optically imprinting” phonons into the gas. A sound wave is a

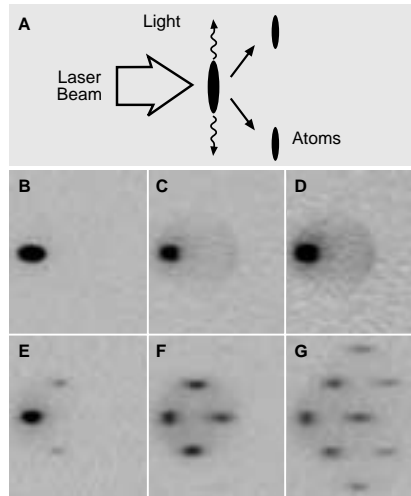
collective excitation of all the atoms in the system and therefore requires that the atoms don't act as individual atoms, but show correlated motion. It has been predicted that this correlated motion results in much weaker light scattering than for free atoms. We found a significant decrease of the rate of light scattering in the phonon regime, providing dramatic evidence for the presence of correlated momentum excitations in the many-body condensate wavefunction [5]. For high-density condensates, even large-angle scattering is in the phonon regime. Therefore, this effect should turn a “pitch-black” condensate transparent since the collective nature of the condensate suppresses its ability to scatter light.



(a) Static structure factor $S(q)$ and (b) shift of the line center from the free particle resonance. $S(q)$ characterizes the strength of the scattering process during which momentum q is transferred to the condensate. As the density and the chemical potential μ increase, the structure factor is reduced, and the Bragg resonance is shifted upward in frequency. Solid lines are predictions of a local-density approximation. Dotted line indicates a mean-field shift of $4\mu/7 \hbar$ as measured in the free-particle regime (shown in open symbols).

6. Superradiant Rayleigh scattering from a Bose-Einstein condensate

We have discovered a new phenomenon in the scattering of light by a condensate: highly directional, “superradiant” scattering of light and atoms [6]. This phenomenon is deeply rooted in the long coherence time of a condensate. When a condensate has scattered light, an imprint is left in the form of long-lived excitations. This “memory” accelerates the scattering of further photons into the same directions. It provides a gain mechanism for the generation of directed beams of atoms and light.

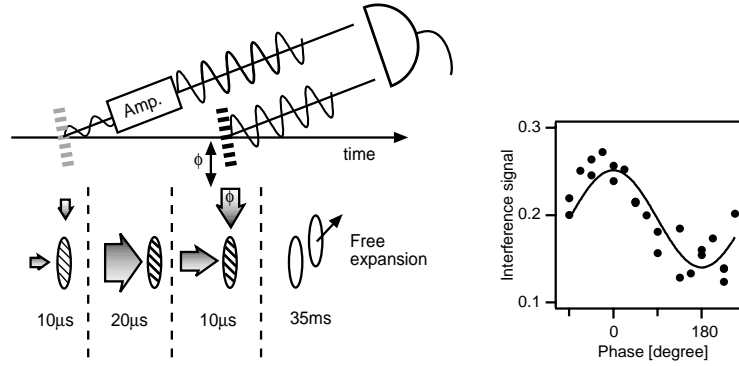


Observation of superradiant Rayleigh scattering. (a) A cigar-shaped condensate is illuminated with a single off-resonant laser beam. Collective scattering leads to photons scattered predominantly along the axial direction, and atoms at 45 degrees. (b-g) Absorption images after 20 ms time-of-flight show the atomic momentum distribution after exposure of the atoms to a laser pulse of variable duration. When the polarization is parallel to the long axis, superradiance is suppressed, and normal Rayleigh scattering was observed (b-d). For perpendicular polarization, directional superradiant scattering of atoms was observed (e-g), and evolved to repeated scattering for longer laser pulses (f,g). The pulse durations are 25 μs (b), 100 μs (c,d), 35 μs (e), 75 μs (f), 100 μs (g). The field of view of each image is 2.8 mm x 3.3 mm. The scattering angle appears to be larger than 45 degrees due to the angle of observation. All images use the same gray scale except for (d), which enhances the small signal of Rayleigh scattered atoms in (c).

This phenomenon is fairly dramatic. When a condensate was illuminated with a single weak laser beam, it randomly scattered light into all directions (with the well-known dipolar pattern – this is ordinary Rayleigh scattering). However, above a certain threshold intensity, the condensate produced two highly directional beams of light. Such highly directional light scattering was accompanied by the production of highly directional beams of recoiling atoms (see figure). These beams of atoms were shown to build up by matter wave amplification. The condensate acted as an amplifier for a recoiling atom and “amplified” it to about a million atoms. If one had collected the light in an optical cavity, one would have realized an optical laser. Therefore, the simultaneous superradiant emission of light and atoms emphasizes the symmetry between atom lasers and optical lasers.

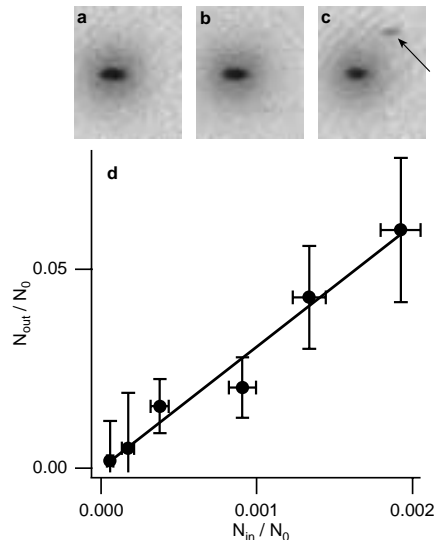
7. Phase-coherent amplification of matter waves

Atom amplification differs from light amplification in one important aspect. Since the total number of atoms is conserved (in contrast to photons), the active medium of a matter wave amplifier has to include a reservoir of atoms. One also needs a coupling mechanism which transfers atoms from the reservoir to an input mode while conserving energy and momentum. We have used the matter wave superradiance which we observed in a BEC [6] to realize a matter wave amplifier [7] (see figure).



Experimental scheme for observing phase coherent matter wave amplification. A small-amplitude matter wave was split off the condensate by applying a pulse of two off-resonant laser beams (Bragg pulse). This input matter wave was amplified by passing it through the condensate pumped by a laser beam. The coherence of the amplified wave was verified by observing its interference with a reference matter wave, which was produced by applying a second (reference) Bragg pulse to the condensate. The interference signal was observed after 35 ms of ballistic expansion. The fringes on the right side show the interference between the amplified input and the reference matter wave.

The gain process can be explained in a semiclassical picture. The input matter wave of wave vector \mathbf{K}_j interferes with the condensate at rest and forms a moving matter wave grating which diffracts the pump light with wave vector \mathbf{k}_0 into the momentum and energy conserving direction $\mathbf{k}_i = (\mathbf{k}_0 - \mathbf{K}_j)$. The momentum imparted by the photon scattering is absorbed by the matter wave grating by coherently transferring an atom from the condensate into the recoil mode, which is the input mode. The rate of scattering, which is given by the square of the grating amplitude, is proportional to the number of atoms in the input mode N_j , implying an exponential growth of N_j (as long as one can neglect the depletion of the condensate at rest).



Input-output characteristic of the matter-wave amplifier. (a-c) Typical time-of-flight absorption images demonstrating matter wave amplification. The output of the seeded amplifier (c) is clearly visible, whereas no recoiling atoms are discernible in the case without amplification (a) or amplification without the input (b). The size of the images is 2.8 mm x 2.3 mm. (d) Output of the amplifier as a function of the number of atoms at the input. A straight line fit shows a number gain of 30.

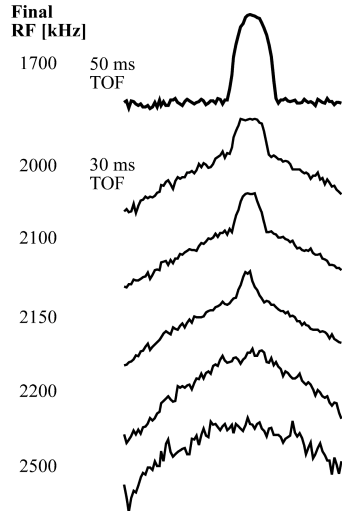
Input matter waves with a well defined momentum were generated by using Bragg scattering to transfer a small part of the condensate into a recoil mode. The input matter wave was amplified by applying an intense radial pump pulse for 20 μ s. The number of atoms in the recoil mode was then determined by suddenly switching off the trap and

observing the ballistically expanding atoms after 35 ms of time-of-flight using resonant absorption imaging. After the expansion, the condensate and the recoiling atoms were fully separated (see figure). Phase-coherence of the matter-wave amplifier was demonstrated with an interferometric technique (see figure).

Our experiment can be regarded as a demonstration of an active atom interferometer. It realizes a two-pulse atom interferometer with phase-coherent amplification in one of the arms. Such active interferometers may be advantageous for precise measurements of phase shifts in highly absorptive media, e.g. for measurements of the index of (matter wave) refraction when a condensate passes through a gas of atoms or molecules [8]. Since the most accurate optical gyroscopes are active interferometers [9], atom amplification might also play a role in future matter-wave gyroscopes [10]. In an independent effort a group at the University of Tokyo [11] has achieved similar results on the amplification of matter waves.

8. A new BEC experiment

A major effort of our group was the design and construction of an improved source of Bose condensed atoms. The design includes an intense slow atomic beam, a glass trapping chamber and a tightly confining magnetic trap. In January '99, the first condensates were produced with about five million atoms in the condensate. A YAG laser with a rapidly scanning x/y deflector was implemented which will allow flexible manipulation and optical trapping of Bose condensates.

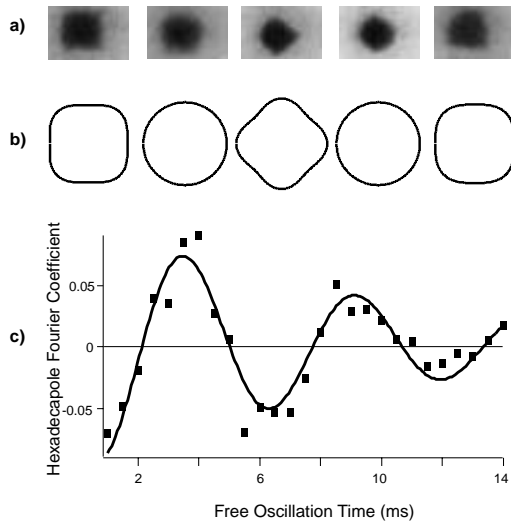


Evidence for Bose-Einstein condensation in our new experiment. As the temperature of the cloud is reduced, the profiles of the ballistically expanding cloud show the sudden appearance of a narrow peak – the condensate. Further cooling produces almost pure condensates. The temperature is almost linearly related to the final rf frequency.

9. Surface excitations in a Bose-Einstein condensate

Collective modes which have no radial nodes and are localized close to the surface of the condensate are called surface modes. In a semiclassical picture these excitations can be considered the mesoscopic counterpart to tidal waves at the macroscopic level. Those excitations are of special interest since they show a crossover between collective and single-particle behavior, which is crucial for the existence of a critical rotational velocity. Furthermore, they probe the surface region of the condensate where the density of the

thermal cloud is peaked, and should be sensitive to the interactions between condensed and non-condensed atoms [12].



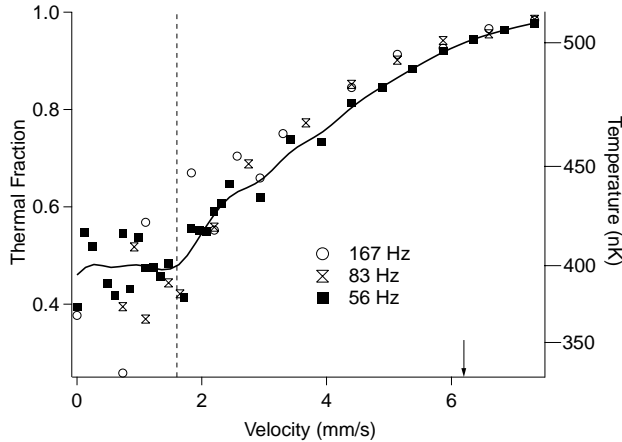
Observation of a standing hexadecapolar excitation of a Bose-Einstein condensate. Absorption images of a condensate driven to excite the $m=4$ mode for various hold times (1, 2, 3.5, 4.5 and 6.5 ms from left to right) in the magnetic trap (a). The shape oscillations of a pure $m=4$ mode are schematically depicted in (b) for one cycle. The contours of images like those in Fig. a were Fourier analyzed. Fig. c shows the oscillation of the $m=4$ Fourier coefficient

Since these modes don't have cylindrical symmetry, they cannot be excited by modulating currents in the coils of a dc magnetic trap. We have therefore developed a method to create perturbations with high spatial and temporal control [13]. Excitations were driven by the optical dipole force of a far-off-resonant focused laser beam which was controlled by a two-axis acousto-optical deflector. A rapid scan created a pattern of two or four points which had the correct symmetry to excite quadrupolar or hexadecapolar surface oscillations. A temporal modulation of the intensity or a rotation of the whole pattern resulted in standing and rotating waves, respectively (see figure).

This novel method should be useful for exciting even higher-lying excitations. It was subsequently used to impart angular momentum to the whole condensate which resulted in vortex formation [14].

10. Evidence for a critical velocity in a Bose-Einstein condensate

The existence of a macroscopic order parameter implies superfluidity of gaseous condensates. Observing frictionless flow is a challenge given the small size of the system and its metastability. We have taken a step towards this goal by studying dissipation when an object was moved through the condensate [15]. This is in direct analogy with the well-known argument by Landau [16] and the vibrating wire experiments in superfluid helium [17]. Instead of dragging a massive macroscopic object through the condensate we used a blue detuned laser beam which repelled atoms from its focus to create a moving boundary condition.



Evidence for a critical velocity. Shown is the final temperature after a laser beam was scanned through the condensate at variable velocity for 900 ms using different scan frequencies. The dashed line separates the regimes of low and high dissipation. The peak sound velocity is marked by an arrow. The data series for 83 and 167 Hz showed large shot-to-shot fluctuations at velocities below 2 mm/sec. The solid line is a smoothing spline fit to the 56 Hz data set to guide the eye.

The beam created a “hole” with a diameter of 13 μm which was scanned back and forth along the long axis of the cigar-shaped condensate (Thomas-Fermi diameters of 45 and 150 μm in the radial and axial directions, respectively). After exposing the condensate to the scanning laser beam for about one second, the final temperature was determined. As a function of the velocity of the scanning beam, we could distinguish two regimes of heating separated by a critical velocity. For low velocities, no or little dissipation was observed, and the condensate appeared immune to the presence of the scanning laser beam. For higher velocities, the heating increased, until at a velocity of about 6 mm/s the condensate was almost completely depleted after the stirring. The cross-over between these two regimes was quite pronounced and occurred at a velocity of about 1.6 mm/s which was a factor of roughly four smaller than the speed of sound at the peak density of the condensate (see figure).

These observations are in qualitative agreement with numerical calculations based on the non-linear Schrödinger equation which predict that heating at subsonic velocities is due to the onset of vortex nucleation [18-20]. Because of surface effects and the non-zero temperature, we expect additional corrections leading to dissipation at even lower velocities and a smooth crossover between low and high dissipation. More precise measurements of the heating should allow us to study these finite-size and finite-temperature effects.

1. J. Stenger, S. Inouye, M.R. Andrews, H.-J. Miesner, D.M. Stamper-Kurn, and W. Ketterle, *Phys. Rev. Lett.* **82**, 2422 (1999).
2. H.-J. Miesner, D.M. Stamper-Kurn, J. Stenger, S. Inouye, A.P. Chikkatur, and W. Ketterle, *Phys. Rev. Lett.* **82**, 2228 (1999).
3. D.M. Stamper-Kurn, H.-J. Miesner, A.P. Chikkatur, S. Inouye, J. Stenger, and W. Ketterle, *Phys. Rev. Lett.* **83**, 661 (1999).
4. J. Stenger, S. Inouye, A.P. Chikkatur, D.M. Stamper-Kurn, D.E. Pritchard, and W. Ketterle, *Phys. Rev. Lett.* **82**, 4569 (1999).
5. D.M. Stamper-Kurn, A.P. Chikkatur, A. Görlitz, S. Inouye, S. Gupta, D.E. Pritchard, and W. Ketterle, *Phys. Rev. Lett.* **83**, 2876 (1999).
6. S. Inouye, A.P. Chikkatur, D.M. Stamper-Kurn, J. Stenger, D.E. Pritchard, and W. Ketterle, *Science* **285**, 571 (1999).
7. S. Inouye, T. Pfau, S. Gupta, A.P. Chikkatur, A. Görlitz, D.E. Pritchard, and W. Ketterle, *Nature* **402**, 641 (1999).

8. J. Schmiedmayer, M.S. Chapman, C.R. Ekstrom, T.D. Hammond, S. Wehinger, and D.E. Pritchard, *Phys. Rev. Lett.* **74**, 1043 (1995).
9. G.E. Stedman, *Rep. Prog. Phys.* **60**, 615 (1997).
10. T.L. Gustavson, P. Bouyer, and M.A. Kasevich, *Phys. Rev. Lett.* **78**, 2046 (1997).
11. M. Kozuma, Y. Suzuki, Y. Torii, T. Sugiura, T. Kuga, E.W. Hagley, and L. Deng, *Science* **286**, 2309 (1999).
12. F. Dalfovo, S. Giorgini, M. Guilleumas, L.P. Pitaevskii, and S. Stringari, *Phys. Rev. A* **56**, 3840 (1997).
13. R. Onofrio, D.S. Durfee, C. Raman, M. Köhl, C.E. Kuklewicz, and W. Ketterle, *Phys. Rev. Lett.* **84**, 810 (2000).
14. K.W. Madison, F. Chevy, W. Wohlleben, and J. Dalibard, *Phys. Rev. Lett.* **84**, 806 (2000).
15. C. Raman, M. Köhl, R. Onofrio, D.S. Durfee, C.E. Kuklewicz, Z. Hadzibabic, and W. Ketterle, *Phys. Rev. Lett.* **83**, 2502 (1999).
16. K. Huang, *Statistical Mechanics*, second edition (Wiley, New York, 1987).
17. C.A.M. Castelijns, K.F. Coates, A.M. Guénault, S.G. Mussett, and G.R. Pickett, *Phys. Rev. Lett.* **56**, 69 (1985).
18. T. Frisch, Y. Pomeau, and S. Rica, *Phys. Rev. Lett.* **69**, 1644 (1992).
19. C. Huepe and M.-E. Brachet, *C.R. Acad. Sci. Paris Série II* **325**, 195 (1997).
20. T. Winiecki, J.F. McCann, and C.S. Adams, *Phys. Rev. Lett.* **82**, 5186 (1999).